Selective oxidation of bulky organic sulphides over lamellar titanosilicate catalysts

Jan Přech[1]*, Russell E. Morris[2], Jiří Čejka[1]

J. Heyrovský Institute of Physical Chemistry, Academy of Sciences of the Czech Republic, v.v.i., Dolejškova 3, CZ-182 23 Prague 8, Czech Republic

[2]EaStCHEM School of Chemistry, University of St Andrews, St Andrews KY16 9ST, UK

*Corresponding author, e-mail: jan.prech@jh-inst.cas.cz, phone: +420 266 053 856

Abstract

Selective oxidation of sulphides is a straightforward method of preparation of organic sulphoxides and sulphones, which are important chemical intermediates and building blocks of pharmaceuticals and agrochemicals. Oxidation of methylphenyl sulphide (MPS), diphenyl sulphide (Ph_2S), and dibenzothiophene (DBTH) over lamellar titanosilicate catalysts with the **MFI** and **UTL**-derived topology was investigated with hydrogen peroxide as the oxidant. Lamellar titanosilicates combine the advantages of crystalline zeolites and mesoporous molecular sieves due to accessible active sites located on the external surface of their layers. The selectivity of the MPS oxidation to methylphenyl sulphoxide is driven by the diffusion restrictions in the catalyst. A methylphenyl sulphoxide selectivity of 95% at 40% conversion was achieved using the Ti-IPC-1-PI catalyst together with an outstanding TON_{tot} = 1418 after 30 min. The selectivity can be adjusted also by dosing of the oxidant to keep its concentration low during the reaction. The silica-titania pillared TS-1-PITi catalyst showed the highest potential of the tested catalysts in oxidative desulphuration, easily oxidising the DBTH to dibenzothiothene sulphone.

Keywords

Oxidation, catalysis, sulphide, lamellar titanosilicate, layered TS-1, hydrogen peroxide

1. Introduction

Selective oxidation is one of the important reactions in organic synthesis and selective oxidation of sulphides is a straightforward method of preparation of organic sulphoxides and sulphones. These compounds are known to be valuable intermediates[1] and building blocks of pharmaceuticals[2] and agrochemicals[3]. Furthermore, oxidative desulphuration can represent an alternative route to hydrodesulphuration (HDS); especially, where the sulphur compounds are difficult to remove using the conventional HDS[4].

Although there is a palette of different oxidants (e.g. peroxides, NaOCl, H_5IO_6, $KMnO_4$[5], peroxynitrous acid[6]) and homogenous catalysts (e.g. complexes of titanium[7], vanadium[8], tungsten[9] and zinc[10], borax[11]), which are able to selectively oxidize sulphides to sulphoxides and sulphones, from the engineering point of view it is always convenient to work with a heterogeneous catalyst. Considering heterogeneous oxidation catalysts, titanium based catalysts are one of the first choices. Titanosilicate zeolites are well established catalysts of olefin epoxidation[12, 13, 14, 15], oxidation of alkanes to alcohols and ketones[16], oxidation of aromatic hydrocarbons to phenols[17], oxidation of phenols to quinones[18] ammoxidation[19, 20] and oxidation of amines to hydroxylamines[21] with hydrogen peroxide and organic hydroperoxides. Last but not least, the titanosilicate ability to catalyse the oxidation of thioethers to sulfoxides is also known[22]. The use of H_2O_2 as the oxidant is highly convenient from both the economic and environmental point of view because it has high content of the active oxygen and the only by-product is water.

Hulea et al. demonstrated that titanosilicates Ti-**BEA** and Ti-**MFI** (TS-1) are active catalysts in the sulphoxidation of dialkyl thioesters with hydrogen peroxide[22]. Thioesters bearing short linear substituents (methyl, ethyl, *n*-butyl) were oxidised rapidly (conversion over 75% after 2 h at 30°C). However, the diffusion limitations of the conventional titanosilicates manifested in the case of diphenyl sulphide (conversion 5 – 38 % after 2h at 30°C, depending on the solvent and catalyst) and methyl-*tert*-butyl sulphide (conversion over TS-1 46% after 2h at 30°C). Corma et al. reported oxidation of methylphenyl sulphide and methyl-*iso*-pentyl sulphide over Ti-**BEA** and Ti-MCM-41 (a mesoporous catalyst) with both hydrogen peroxide and *tert*-butylhydroperoxide[23]. The Ti-MCM-41 provided higher conversion (30% after 2h) of methyl-*iso*-pentyl sulphide then the Ti-**BEA** (18%) although for methylphenyl sulphide it was *vice versa* (80% vs. 95% after 0.5 h), confirming the importance of diffusion limitations influence on the reaction. Trukhan et al. compared Ti-MCM-41 with other mesoporous titanosilicate Ti-SBA-15 demonstrating the largest disadvantage of the mesoporous titanosilicates: low titanium dispersion and high thickness of the wall, which leads to part of the titanium centres remaining inaccessible[24]. Recently, Kon et al. investigated dialkyl and alkyl-aryl sulphides over Ti-**MWW** (titanosilicate analog of MCM-22) material and Ti-IEZ-**MWW** (interlayer expanded zeolite). Especially for the bulkiest diphenyl sulphide, the decrease in the diffusion restrictions provided by the interlayer expansion was clearly revealed (conversion over Ti-**MWW** 36% vs. Ti-IEZ-**MWW** 64% after 18 h at 40°C)[25]. Encouraged by these findings, we turned our attention towards the use of lamellar titanosilicate catalysts with **MFI** (layered and pillared TS-1) and **UTL**-derived (denoted Ti-IPC-1-PI) topology as catalysts of the bulky sulphides oxidation.

In general, lamellar materials combine the advantages of crystalline zeolites and mesoporous molecular sieves. They possess well-defined active centres, characteristic of highly crystalline

materials, on one hand and they provide easy accessibility of the active sites located on the outer surface of the layers on the other hand. There are three basic approaches to the preparation of lamellar zeolitic materials[26]: (i) Some zeolites (e.g. **MWW**, **FER**) form lamellar precursors, which condense into fully connected zeolitic framework upon calcination.[27, 28] (ii) Lamellar zeolites (e.g. **MFI**) can be prepared using specially designed templates, which restrict the crystal growth in one of the crystallographic directions.[29] (iii) Some germanosilicate zeolites (e.g. **UTL**, **IWW**) have the form of dense silica layers connected by double 4-ring (D4R) units. Germanium is preferentially located in these D4R units making centres of instability in the framework. The germanium D4R can be hydrolysed under mild acidic medium leaving the crystalline silica layers of a unit cell thickness intact.[30, 31]

In this paper, we report on oxidation of various bulky sulphides (methylphenyl sulphide, diphenyl sulphide and dibenzothiophene) over lamellar crystalline titanosilicate catalysts under mild conditions with hydrogen peroxide as the oxidant. The discussed catalysts are synthesized by the latter two methods of lamellar zeolite preparation i.e. surfactant templated synthesis[32] (layered and pillared TS-1) and D4R units hydrolysis[33] (Ti-IPC-1-PI). The results are compared with standard TS-1 and Ti-**UTL** catalyst.

2. Experimental

2.1. Synthesis of conventional TS-1

Conventional titanosilicates TS-1 (TS-1) were prepared from a gel with initial Si/Ti ratio 43 using the procedure originally described in Ref. 34 with slight modifications. Tetrabutyl orthotitanate (TBOTi, Aldrich, 97%) and tetraethyl orthosilicate (TEOS, Aldrich, 98%) were used as the titanium and silica source, respectively. Tetrapropylammonium hydroxide (Aldrich, 40 wt. % in water) served as a structure directing agent (SDA). The initial gel composition was 100 TEOS: 2.32 TBOTi : 35 SDA : 4000 H_2O. Materials with two different crystal sizes were obtained by adjusting the hydrothermal crystallization time to 70 h (TS-1 (200)) or 94 h (TS-1 (600)) in a 90 ml Teflon-lined autoclave at 175°C under agitation. The final zeolite was centrifuged, washed with water, dried at 80°C and finally calcined in air, at 550°C for 8 h, using a temperature ramp of 1°C/min.

2.2. Synthesis of layered and pillared TS-1

The synthesis of parent layered TS-1 was carried out according to the Na et al. procedure[32] from TEOS and TBOTi, using surfactant SDA $C_{18}H_{37}$-$N^+(CH_3)_2$-C_6H_{12}-$N^+(CH_3)_2$-C_6H_{13} in hydroxide form ($C_{18\text{-}6\text{-}6}OH_2$; prepared as described in the literature[32]). The TBOTi was added dropwise into TEOS and stirred

for 30 minutes. Then an aqueous solution of the SDA was added to the mixture. The synthesis mixture with initial composition 100 TEOS: 2.5 TBOTi : 6 $C_{18\text{-}6\text{-}6}OH_2$: 5000 H_2O was hydrolysed at 60°C for 3 h. The evaporated mass of ethanol and water were replaced with the same mass amount of water at the end. The final gel hydrothermally crystallized in a 90 ml Teflon-lined autoclave at 160°C for 236 h under agitation. After the given time, the zeolite was filtered off, washed with water, dried at 80°C and finally calcined or subjected to the pillaring treatment. Calcination was carried out at 570°C for 8 h, using a temperature ramp of 1°C/min.

The silica and silica-titania pillaring procedures for the layered TS-1 were performed using our previously reported procedures[35]. Dry as-synthetized layered TS-1 was dispersed in TEOS (TS-1-PISi) or a mixture of TEOS and TBOTi (TS-1-PITi) in Si/Ti molar ratio 60 (10 g of the TEOS/1 g of the zeolite) and stirred at 65°C for 24 h. Then the mixture was centrifuged and the solid material was dried for 48 h at room temperature. The dry product was hydrolysed in water with 5% of ethanol (100 ml/1 g) at ambient temperature for 24 h under vigorous stirring. At the end, the zeolite was centrifuged again, dried at 65°C and calcined in air, at 550° C for 10 h, using the temperature ramp of 2° C/min.

2.3. Synthesis of Ti-UTL and related Ti-IPC-1-PI and Ti-IPC-2

The preparation procedures for the Ti-**UTL**, Ti-IPC-1-PI and Ti-IPC-2 are described and discussed in our previous paper[36]. The initial gel for the Ti-**UTL** was prepared from Cab-O-Sil M5 silicon oxide (Havel Composites, Czech Republic), TBOTi, germanium oxide (Alfa Aesar, Germany, 99.999%), distilled water, and (6R,10S)-6,10-dimethyl-5-azoniaspiro[4.5]decane hydroxide in the role of an SDA (the SDA preparation is described in Ref. 37). Cab-O-Sil M-5 and GeO_2 were added to an aqueous solution of the SDA under stirring. After 30 minutes of homogenization, TBOTi, dilluted 1:3 with 1-butanol, was added dropwise and the gel was stirred for another 30 minutes. The initial molar composition of the synthesis gel was 2 TBOTi : 50 GeO_2 : 50 SDA : 100 SiO_2 : 3750 H_2O. The zeolite crystallized in a 90-ml Teflon-lined autoclave at 175°C for 420 h under agitation. The final product was filtered, washed with water, dried at 85°C and calcined in air. The temperature program of the calcination was 200°C for 2 h, then 350°C for 4 h and finally 550°C for 8h, using a temperature ramp of 2°C/min.

The Ti-IPC-1-PI[33] and Ti-IPC-2[30] materials were prepared by the post-synthesis modification of the calcined Ti-**UTL**. The Ti-**UTL** was converted into lamellar precursor Ti-IPC-1P by hydrolysis of the germanium D4R units with 0.01 M HCl (250ml/g) at 75°C for 16 h under agitation. The resulting lamellar precursor Ti-IPC-1P was collected by filtration, washed with water, dried at 65°C and subjected to the pillaring to form Ti-IPC-1PI or silylation to form Ti-IPC-2.

To prepare the Ti-IPC-1PI, the precursor Ti-IPC-1P was swollen with a solution of cetyltrimethylammonium hydroxide (CTMA OH, 25 wt. % in water, 30 g/g of the zeolite). The swelling occurred at room temperature for 24 h under stirring. The swollen product was centrifuged, washed with water and dried at 65°C. The pillaring was done in the same way as for the layered TS-1. Pure TEOS was used only (10ml/g of the swollen Ti-IPC-1P, *vide supra*).

The Ti-IPC-2 catalyst was prepared by silylation of the Ti-IPC-1P with diethoxydimethylsilane in 1M HNO_3 in a 25-ml Teflon-lined autoclave at 175°C for 16 h without agitation. Typically, 10 ml of the HNO_3 solution and 0.5 g of the diethoxydimethylsilane were used per 1 g of the Ti-IPC-1P. A strongly hydrophobic product was collected by filtration, dried and calcination at 550°C for 8 h using a temperature ramp of 2°C/min.

2.4. Characterization techniques

X-ray powder diffraction (XRD) patterns were collected using a Bruker AXS D8 Advance diffractometer equipped with a graphite monochromator and a position sensitive detector Våntec-1 using CuKα radiation in Bragg–Brentano geometry. Data were collected in continuous mode over the 2θ range of 1-40° for the lamellar materials and 2θ range of 5-40° for the conventional zeolites with a step size of 0.00853° and time per step 0.25 s.

The textural properties were determined from nitrogen sorption isotherms. The isotherms were measured at liquid nitrogen temperature (-196°C) with Micromeritics Gemini volumetric instrument. Prior to the sorption measurements, individual zeolites were outgassed in a stream of helium at 300°C for 3 h.

BET area was evaluated using adsorption data in the range of a relative pressure from $p/p_0 = 0.05$ to $p/p_0 = 0.20$. The t-plot method[38] was applied to determine the volume of micropores (V_{micro}). The adsorbed amount of nitrogen at $p/p_0 = 0.95$ reflects the total adsorption capacity (V_{total}) of the material.

DR-UV/Vis absorption spectra were collected using Perkin-Elmer Lambda 950 Spectrometer with 2mm quartz tube and large 8 x 16 mm slit. The data were collected in the wavelength range of 190-500 nm. All the samples were analyzed after calcination.

Chemical composition of the materials (expressed hereafter as a Si/Ti ratio) was determined by ICP-OES ThermoScientific iCAP 7000 instrument.

2.5. Catalytic tests

The oxidations of methylphenyl sulphide (MPS, Aldrich, 99 %) and allylphenyl sulphide (APS, Aldrich, 96.5 %) were carried out in a 25 ml magnetically stirred glass three-necked round bottom flask equipped with a Dimroth condenser at 30°C. Typically, 8 mmol of the sulphide was dissolved in 10 ml of acetonitrile (Fisher chemical, HPLC grade) together with 250 µl of 1,3-diisopropylbenzene (internal standard, Fluka, 95%) and 50 mg of the catalyst were introduced into the mixture. For MPS, this setup corresponds to substrate/catalyst mass ratio S/C = 20. The mixture was heated to the reaction temperature and the reaction was started by addition of H_2O_2 aqueous solution (Aldrich, 35 wt. %). Typically, the sulphide/H_2O_2 molar ratio was 2.

The oxidations of diphenyl sulphide (Ph_2S, Aldrich, 98 %) and dibenzothiophene (DBTH, Aldrich, 98 %) were carried in a similar setup at 40°C. In the case of Ph_2S, 4 mmol of Ph_2S were mixed with 10 ml of acetonitrile, 250 µl of 1,3-diisopropylbenzene and 50 mg of the catalyst (S/C = 15) and the reaction was started by the addition of 4 mmol of H_2O_2 aqueous solution (sulphide/H_2O_2 = 1). In case of DBTH, 2 mmol of the substrate were dissolved in 15 ml of acetonitrile together with 125 µl of 1,3-diisopropylbenzene and 25 mg of the catalyst (S/C = 15) and the reaction was started by the addition of 2 mmol of H_2O_2 aqueous solution (sulphide/H_2O_2 = 1). The higher dilution in the case of DBTH was used to prevent crystallisation of the DBTH and products out of the samples while cooled.

Samples of the reaction mixture were taken in regular intervals, immediately centrifuged, cooled and analysed using an Agilent 6850 GC system with 50 m long DB-5 column, an autosampler and a FID or an MS detector. Helium was used as a carrier gas. The internal standard calibration method was used for the evaluation of the kinetic data.

3. Results and discussion

3.1. Catalyst description and characterization

The layered and pillared TS-1 catalysts preparation is based on the surfactant templated synthesis approach, where the growth of the crystals is restricted by long hydrophobic chains of the template[32]. As a result, lamellar material consisting of **MFI** layers approximately 2 nm thick is formed[32]. The layers are not perfectly uniform (do not fit perfectly one on another) because each of them is, in fact, a single crystal. Therefore, the layered TS-1 preserves some slit-shaped mesopores (in contrast to the D4R hydrolysed lamellar materials[33]) even after calcination.

The XRD patterns of the TS-1 based catalysts are presented in Figure 1. The conventional TS-1 catalysts (denoted TS-1 (200) and TS-1 (600) according to their typical crystal size determined form

SEM images) possess the XRD patterns, which are characteristic for the materials with **MFI** topology. The pattern of the layered TS-1 is consistent with that for nanosheet TS-1 observed by Na et al.[32] In the low 2θ region, a diffraction line on 2θ = 1.5° can be observed because the layers preserved some regular orientation even after calcination; however, usually this diffraction line is not present after calcination. To keep the layer apart and to enhance the active sites accessibility, the so-called pillaring treatment[35] is used. A part of the interlayer space is filled with amorphous mesoporous silica (TS-1-PISi) or silica-titania (TS-1-PITi) and the material keeps its original morphology even after calcination. For the TS-1-PISi and TS-1-PITi, a strong diffraction line is present on 2θ = 1.7°. This line characterizes the regular organization of the layers in the pillared material. The position of the line corresponds to d-spacing of 4.5 nm and interlayer distance of 2.5 nm. The titanium source (1.7 %) was added into the pillaring medium to impregnate the layers with additional Ti sites to suppress the active phase dilution by the amorphous pillars[35].

Figure 1: Powder XRD patterns of the TS-1 based catalysts. From the top: TS-1 (200), TS-1 (600), layered TS-1, TS-1-PISi, TS-1-PITi.

The synthesis and post-synthesis modifications of the Ti-**UTL** are thoroughly discussed in our previous paper[36]. The XRD patterns of the Ti-**UTL**, Ti-IPC-1-PI and Ti-IPC-2 are presented in Figure 2. The Ti-IPC-2 is a zeolite with OKO topology[39], which was prepared by stabilization of the Ti-IPC-1P (lamellar precursor formed by the germanium D4R hydrolysis) with diethoxydimethylsilane. The process of the **UTL** to **OKO** transformation, so-called ADOR process, is intensively studied by our group[30]. A shift of the most intensive 200 diffraction line of the **UTL** towards lower angles can be observed after the transformation to Ti-IPC-1-PI, indicating the extension of the d-spacing form 2.9 nm to 3.7 nm (note that the intensity of 200 line decreases in Ti-IPC-1-PI pattern and the 100 line is the most intense). On the other hand, the 200 line is shifted towards higher angles for Ti-IPC-2 material, where the interlayer distance decreases in comparison with Ti-**UTL** (d-spacing 2.3 nm).

Figure 2: Powder XRD patterns of the UTL based catalysts. From the top: Ti-IPC-2, Ti-IPC-1-PI, Ti-UTL.

The textural properties obtained by N_2 sorption isotherms analysis at -196°C together with the titanium content (expressed as Si/Ti molar ratio) are summarized in Table 1. The conventional TS-1 (200), TS-1 (600) and layered TS-1 catalysts exhibit BET areas between 450 and 528 m^2/g. The total adsorption capacity (V_{tot}) increased from 0.16 cm^3/g of the TS-1 (600) to 0.30 cm^3/g by the decrease in the crystal size due to increase in the interparticle volume. The lamellar material possesses lower

micropore volume (V_{mic} = 0.09 cm^3/g) in comparison with the conventional TS-1 (V_{mic} = 0.15 resp. 0.13 for TS-1 (200) and TS-1 (600)). Therefore, the Ti sites are expected to be better accessible in the lamellar material.

The pillaring treatment led to an increase in both BET area (TS-1-PISi: 575 m^2/g, TS-1-PITi: 685 m^2/g) and total adsorption capacity (TS-1-PISi: 0.39 cm^3/g, TS-1-PITi: 0.37 cm^3/g). The decrease in the Ti content in the TS-1-PISi material (Si/Ti=55 vs. layered TS-1 Si/Ti=36) can be compensated by the silica-titania pillaring (TS-1-PITi Si/Ti=31).

Similarly, the hydrolysis and transformation of the Ti-**UTL** into the Ti-IPC-1-PI material led to a strong increase in both BET area (Ti-**UTL**: 539 m^2/g, Ti-IPC-1-PI: 1001 m^2/g) and adsorption capacity (Ti-**UTL**: 0.29 cm^3/g, Ti-IPC-1-PI: 0.67 cm^3/g). The Ti-IPC-1-PI has no micropores because there are no channels running through the crystalline layers. Contrary to Ti-IPC-2, where the BET area (383 m^2/g), micropore volume (0.15 cm^3/g), and adsorption capacity (0.29 cm^3/g) decreased in comparison with Ti-**UTL** due to the reduction of the size of channels (from 14x12-ring (**UTL**) to 12x10-ring (**OKO**)). The decrease in the titanium content form Si/Ti=138 (Ti-**UTL**) to Si/Ti=210 (Ti-IPC-2) and Si/Ti=480 (Ti-IPC-1-PI) suggests that the titanium is homogenously distributed through the Ti-**UTL**. In the case of Ti-IPC-2, the D4R units (apparently containing some Ti atoms in addition to germanium) are removed and replaced by the silica S4R units. In the case of Ti-IPC-1-PI, the D4R are removed and the crystalline material is diluted with the silica pillars. Nevertheless, both materials are catalytically active (*vide infra)*.

Table 1: Textural properties and Ti content of the lamellar and conventional titanosilicate catalysts under study.

Titanosilicate	BET (m^2/g)	V_{mic} (cm^3/g)	V_{meso} (cm^3/g)	V_{tot} (cm^3/g)	Si/Ti
TS-1 (600)[a]	450	0.13	0.03	0.16	39
TS-1 (200)[a]	528	0.15	0.16	0.31	36
lam TS-1	473	0.09	0.21	0.30	36
TS-1-PISi	575	0.10	0.29	0.39	55
TS-1-PITi	685	0.07	0.30	0.37	31
Ti-UTL	539	0.24	0.05	0.29	139
Ti-IPC-1-PI	1001	0	0.67	0.67	480
Ti-IPC-2	383	0.15	0.07	0.22	210

[a] The number in brackets expresses a typical crystal size in nm determined from SEM.

To characterise the titanium sites, the DR-UV-Vis spectra were recorded for all the catalysts. The spectra of the TS-1 based materials are presented in Figure 3 and the spectra of the **UTL**-based catalysts are shown in Figure 4. The main feature in all the spectra is a band centred around 210 nm. Furthermore, some absorption between 260 and 300 nm is observed in the spectra of TS-1-PISi, TS-1-PITi, Ti-UTL and Ti-IPC-2. No absorption around 330 nm is observed except of the TS-1 (200) sample. Zecchina et al.[40] and Wu et al.[41] ascribed the band at 210 nm to tetrahedrally coordinated framework $Ti(OSi)_4$ species. The absorption between 260-290 nm results from the presence of 5- and 6-coordinated extra-framework titanium species[42]. The absorption above 300 nm is characteristic for the anatase TiO_2 phase, which is known to ineffectively decompose the hydrogen peroxide; however, with the exception of some traces in the TS-1 (200), it is not present in the discussed catalysts.

Figure 3: DR-UV-Vis spectra of the TS-1 (200) (a), TS-1 (600) (b), layered TS-1 (c), TS-1-PISi (d), TS-1-PITi (e).

Figure 4: DR-UV-Vis spectra of the Ti-UTL (a), Ti-IPC-1-PI (b) and Ti-IPC-2 (c).

3.2. Oxidation of methyl phenyl sulphide

The TS-1 based catalysts and the Ti-**UTL** derived catalysts were used in oxidation of methylphenyl sulphide (MPS) with aqueous hydrogen peroxide as the oxidant in acetonitrile at 30°C. The conversion curves using the TS-1 based catalysts are given in Figure 5 and the product distribution, selectivity and TON are summarized in Table 2. The MPS was chosen being one of the most common model substrates to study oxidation of organic sulphides. A blank experiment revealed that the reaction without catalyst occurs only slowly (conversion of 2.5% after 120 min) under the experimental conditions. Therefore, the observed kinetic profiles can be ascribed to the catalysts. The maximum theoretical conversion is 50% under the used conditions. In all the cases, the reaction started rapidly and slowed down as the hydrogen peroxide was running out until it stops at the 100% conversion of H_2O_2. When fresh H_2O_2 was added, the reaction was restored.

The TS-1 (600) catalyst gave the lowest conversion (11% after 30 min) and the least selective (75 % at 25% conversion) of the TS-1 based catalysts. The use of a catalyst with smaller crystals resulted in an increase in the conversion (21% after 30 min) due to shorter diffusion paths. The use of lamellar catalysts led to another strong increase in the conversion: TS-1-PISi 26% < layered TS-1 36% < TS-1-PiTi 41% after 30 min. Among the lamellar TS-1 catalysts, it appears that the conversion is more dependent on the titanium content than on the textural properties.

To compare the intrinsic activity of the catalysts, TON values were calculated after 30 min of the reaction (Table 2). There are two different TON presented. The primary TON (TON_{prim}) includes only the oxidation of MPS to methylphenyl sulphoxide (MPSO); however, the consecutive oxidation of MPSO to methylphenyl sulphone ($MPSO_2$) is also catalysed and therefore is considered. The total TON (TON_{tot}) includes both reactions. The highest TON_{tot} = 151 is observed for the TS-1-PISi possessing the most open structure (V_{tot} = 0.39 cm^3/g, V_{micro} = 0.10 cm^3/g). Then the both TON_{prim} and TON_{tot} decrease with decreasing mesopore volume (V_{meso}, estimated as a difference between V_{tot} and V_{mic}): layered TS-1 (V_{meso}=0.21 cm^3/g, TON_{tot}=136) > TS-1 (200) (V_{meso}=0.16 cm^3/g, TON_{tot}=87) > TS-1 (600) (V_{meso}=0.03 cm^3/g, TON_{tot}=60). The TS-1-PITi does not fit into this trend (V_{meso}=0.30 cm^3/g, TON_{tot}=132). This is most probably due to the inaccessibility of a part of the titanium sites located inside the silica pillars.

Figure 5: Catalytic oxidation of methylphenyl sulphide (MPS) over the TS-1 based catalysts at 30°C. Reaction conditions: 8 mmol of MPS, 4 mmol of H_2O_2 (35 wt.%) , 50 mg of catalyst, 250 µl of internal standard, 10 ml acetonitrile, 900 rpm.

The selectivity was determined at 40% conversion. The order of the catalyst selectivity to sulphoxide is the same as in the case of TON: TS-1 (600) (61%) < TS-1 (200) (78%) < layered TS-1 (87%) < TS-1-PISi (91%). The selectivity of the reaction to the sulphoxide is mostly dependent on the diffusion restrictions in the catalyst and partially on the titanium content. The lower diffusion restrictions, the higher sulphoxide selectivity was observed. The assumption of the diffusion driven selectivity is also in accordance with the data reported by Corma et al.[23] and Kon et al.[25] on MPS oxidation. The TS-1-PITi stands again out of the trend (S = 85%). Based on the fact that it is the catalyst providing the highest conversion before the H_2O_2 is consumed, we expect that it has an increased amount of easily accessible active sites in comparison with TS-1-PISi, which were formed post-synthetically during the silica-titania pillaring and thus the TS-1-PITi is less selective than it should be according to its textural properties.

Finally, the efficiency of the hydrogen peroxide used was estimated from the yield of sulphoxide and sulphone at 100% conversion of the H_2O_2 (in the case it was reached during the experiment). For the catalysts TS-1 (200), layered TS-1 and TS-1-PISi (and also for the Ti-**UTL**) it was the same (94-95%). In the case of TS-1-PITi, the efficiency was lower (91%) due to decomposition on the hexacoordinated titanium sites (see the DR-UV-Vis discussion) whose structure might by close to the anatase structure (titanium atoms in anatase are also 6-coordinated).

Table 2: Oxidation of methylphenyl sulphide at 30°C.

Catalyst	Product composition (120 min)[a]		$S_{(40\%)}$ [b]	$E_{(100\%)}$ [c]	TON_{prim} [d]	TON_{tot} [e]
	MPSO (%)	$MPSO_2$ (%)	(%)	(%)	(30 min)	(30 min)
TS-1 (600)	60	40	61 (25%)	n.a.	43	60
TS-1 (200)	74	26	78	94	74	87
layered TS-1	94	6	87	94	127	136
TS-1-PISi	91	9	91	95	137	151
TS-1-PITi	93	7	85	91	124	132
Ti-UTL	96	4	98	95	200	208
Ti-IPC-1-PI	94	6	95	100	1338	1418
Ti-IPC-2	84	16	69 (8%)	n.a.	101	115

[a] Ratio between methylphenyl sulphoxide (MPSO) and methylphenyl sulphone ($MPSO_2$) after 120 min of the reaction.

[b] Methylphenyl sulphoxide selectivity at 40 % conversion; calculated as S = [yield of MPSO]/[conversion of MPS]. Where the conversion of 40 % was not reached during the experiment, the selectivity is given at maximum conversion.

[c] Hydrogen peroxide efficiency at 100% conversion of the H_2O_2; calculated as E = ([yield of MPSO]+ 2 . [yield of $MPSO_2$])/[initial amount of H_2O_2]).

[d] TON of the primary oxidation of MPS; calculated as TON_{prim}=[n(MPS) converted]/[n(Ti)].

[e] Overall TON (encounting the oxidation of MPSO to $MPSO_2$); calculated as TON_{tot} = ([n(MPS) converted]+[n($MPSO_2$) formed])/[n(Ti)].

The conversion curves obtained using the Ti-**UTL** and derived catalysts are presented in Figure 6 together with the curve of TS-1 (600) as a benchmark. All the catalysts (Ti-**UTL**, Ti-IPC-1-PI and Ti-IPC-2) have low titanium content (Si/Ti = 139, 480 and 210 respectively) in comparison with the TS-1 based catalysts (Si/Ti = 31 – 55); however, they possess extra-large and large pores (Ti-UTL possess 14x12 ring 2D-channel system and Ti-IPC-2 12x10 ring channels) and the Ti-IPC-1-PI is purely mesoporous. Therefore, they are expected to have lowed diffusion restrictions in comparison with the TS-1 based catalysts. The Ti-**UTL** gave conversion of 15%, the Ti-IPC-1-PI 29% and Ti-IPC-2 only 5% after 30 min of the reaction. However, when the activity is expressed as the TON, the intrinsic activity of Ti-IPC-2 (TON_{tot} = 115 after 30 min) corresponds to the TS-1 based catalysts (from TON_{tot} = 60 to 151). The Ti-**UTL** and Ti-IPC-1-PI catalysts own an outstanding intrinsic activity, providing TON_{tot} of 208 and 1418, respectively. Furthermore, the Ti-**UTL** is the most selective of the discussed catalysts

(98% at 40% conversion) and the Ti-IPC-1-PI is most efficiently using the H_2O_2 (E = 100%) together with the selectivity of 95%. One could say, that high TON is not important while the catalyst possess only very little of the active centres, but this is not the case of the Ti-IPC-1-PI catalyst. The MPS conversion over this catalyst (29% after 30 min) is fully comparable with the lamellar TS-1 catalysts (e.g. TS-1-PISi: 26%, layered TS-1 36%) at the same conditions.

On the other hand the selectivity of the Ti-IPC-2 is only 69% at 8% conversion and after initial 20 min the conversion increases only slowly (from 5% to 8% between 35 and 180 min of the reaction), this is most probably because the pores are not wide enough and the diffusion restrictions are too severe.

Figure 6: Catalytic oxidation of methylphenyl sulphide (MPS) over the Ti-UTL based catalysts at 30°C. TS-1 (600) is shown as a benchmark. Reaction conditions: 8 mmol of MPS, 4 mmol of H_2O_2 (35 wt.%) , 50 mg of catalyst, 250 µl of internal standard, 10 ml acetonitrile, 900 rpm.

3.3. Driving the selectivity

In the previous section, we have shown that the selectivity of the MPS oxidation depends mainly on the diffusion properties of the catalyst. In this section, we report on the influence of other parameters on the selectivity i.e. the substrate/catalyst ratio (S/C) and the influence of H_2O_2 concentration in the reaction mixture.

The influence of the S/C ratio was investigated using the layered TS-1 catalyst. Based on the high selectivity obtained using the Ti-UTL and Ti-IPC-1-PI catalysts, which have low concentration of the active sites, we expected that the decrease in the amount of the catalyst might influence the selectivity. The Figure 7 presents the obtained conversion curves. When the TON_{prim} in 30 min are calculated, some increase in the intrinsic activity can be observed (S/C=20: 127, S/C=40: 136, S/C=100: 170). The blank experiment showed that the oxidation of MPS occurs also without the presence of the catalyst (Figure 5). Assuming the rate of the non-catalysed oxidation is independent on the amount of catalyst, we conclude that the observed differences result from different proportion between the amounts of MPS converted non-catalytically and total conversion. The selectivity curves of the experiments with different S/C ratio are presented in Figure 8. We can observe that they correspond perfectly to one another, showing the selectivity of 86% at 25% conversion and therefore we conclude the selectivity is not influenced by the used amount of catalyst (S/C ratio).

Figure 7: Conversion curves of MPS oxidation over layered TS-1 using different S/C ratio.

Figure 8: Selectivity curves of MPS oxidation over layered TS-1 using different S/C ratio.

The concentration of the oxidant is another parameter, which can be expected to influence the selectivity in a system of two consecutive oxidation reactions. To investigate this influence, we have chosen two catalysts i.e. TS-1 (600) and layered TS-1 and we conducted the catalytic experiment with 0.5 molar equivalent of H_2O_2 based on the MPS (a standard experiment), with 1 molar equivalent of H_2O_2 and with 5 doses of 0.1 equivalent of H_2O_2 during 5 h. The obtained conversion curves resp. curves showing the development of conversion in the case of the dosing experiment are presented in Figure 9. For the layered TS-1 it can be observed, that in the initial 20 min the reaction rate is the same for 0.5 and 1 eq and at higher conversion, the 0.5 eq reaction starts to fade out. When the hydrogen peroxide is dosed, after each addition, the total conversion is reached within first 20 min and the reaction is restored only after addition of fresh H_2O_2.

Using the TS-1 (600) catalyst, the reaction is faster with the 1 eq of H_2O_2 since the very beginning (conversion 20% after 30 min) of the experiment than in the standard 0.5 eq run (11% after 30 min). In the case of the dosed experiment some steps can be observed on the curve of the increase of the conversion at the beginning (as in the case of layered TS-1); however, total conversion is not reached during the interval between the doses and the curve is smoothing.

The selectivity curves are shown in Figure 10. An increase in the selectivity in the case of 0.1 eq dosing experiment is clearly visible. For the layered TS-1 the selectivity (calculated at 40% conversion) increased upon dosing of the oxidant from 87% (standard experiment) to 91%. Furthermore, considering the rapid conversion of the H_2O_2 dose, we believe that the dosing of the oxidant can be tuned in such way that the selectivity is increased without or only with a slight decrease in the reaction rate. Using 1 eq of H_2O_2 at the beginning of the reaction, the selectivity decreased only slightly to 85%.

For the TS-1 (600) catalyst similar behaviour was observed. The selectivity of the reactions is calculated at 25% conversion; however, the selectivity curves are linear, therefore, the selectivity does not change much over the studied range of conversion. When the oxidant was dosed, the selectivity increased from 61 % (standard experiment) to 65%. When the 1 eq of H_2O_2 was used, it decreased to 56%.

Figure 9: Development of conversion in time using different amount of H_2O_2 and dosing of the oxidant over TS-1 (600) (gray) and layered TS-1 (black).

Figure 10: Selectivity curves of the experiments using different amount of H_2O_2 and dosing of the oxidant over TS-1 (600) (gray) and layered TS-1 (black).

3.4. Oxidation of bulky sulphides

To further demonstrate the potential of the lamellar titanosilicate catalysts, we studied oxidation of two substrates bulkier than the MPS. Table 3 summarises the results of dibenzothiophene (DBTH and diphenyl sulphide (Ph_2S) oxidation. The experiments were conducted at 40°C using molar 1 eq. of the oxidant. The order of the catalysts in terms of conversions and TON is similar to the results obtained in the MPS oxidation.

In the DBTH oxidation, the major product was the dibenzothiophene sulphone ($DBTHSO_2$) contrary to the other substrates. The highest conversion (28% after 240 min) and yield of the $DBTHSO_2$ (24 %)

was obtained over the TS-1-PITi thanks to its well accessible titanium sites formed during the silica-titania pillaring. The layered TS-1 provided conversion of 20% because the DBTF cannot access the micropores in the layers (evidenced by the zero conversion over the TS-1 (600) catalyst) and therefore only a part of the titanium sites located on the outer surface of the layers is active. The Ti-IPC-1-PI catalyst provided conversion of 9.5 % and yield of 7.9 % after 240 min. Among the conventional zeolites, the Ti-**UTL** was the only catalyst, which provided some conversion (3.3 % after 240 min). The TS-1 (600) and Ti-IPC-2 were not active at all (zero conversion after 240 min) because their channels are not wide enough for the DBTH molecule. We conclude, that especially the silica-titania pillared catalysts like TS-1-PITi have the potential to oxidise bulky and rigid molecules like DBTF in the desulphuration processes and the advantages of lamellar titanosilicates in oxidation of bulky sulphides were clearly demonstrated.

The oxidation of diphenyl sulphide (Ph_2S) occurred over all the examined catalysts. Even the TS-1 (600) provided conversion of 22% after 240 min being the most selective (y(Ph_2SO) = 20%, selectivity 93% at 25% conversion). It appears that the Ph_2S is flexible enough to enter the TS-1 micropores; however it is not the case of the diphenylsulphoxide (Ph_2SO) and therefore high selectivity is gained over the catalysts with higher diffusion restrictions. The layered TS-1 provided conversion of 34% at the same time and TS-1-PITi 59%; however, the selectivity over TS-1-PITi was only 85%. The Ti-**UTL** provided conversion similar to the TS-1 (600) with slightly lower selectivity (87% at 25% conversion) and the Ti-IPC-1-PI showed once more an outstanding intrinsic activity (TON_{prim} = 1818 in 240 min) in comparison with the other catalysts (TON_{prim} from 81 (TS-1 (600)) to 287 (Ti-**UTL**)).

Table 3: Oxidation of dibenzothiophene (DBTF) and diphenyl sulphide (Ph_2S).

	Oxidation of DBTF			Oxidation of Ph_2S		
Catalyst	X (240 min)[a] (%)	y ($DBTHSO_2$ 240min)[b] (%)	TON_{prim}[c] (240 min)	X (240min)[a] (%)	y (Ph_2SO, 240 min)[d] (%)	TON_{prim}[e] (240 min)
TS-1 (600)	0	0	0	22	20	81
layered TS-1	20	18	69	34	30	117
TS-1-PITi	28	24	83	59	46	175
Ti-UTL	3.3	2.6	44	23	19	287
Ti-IPC-1-PI	9.5	7.9	438	39	31	1818
Ti-IPC-2	0	0	0	6.3	4.2	127

[a] Conversion of DBTH resp. Ph_2S after 240 min of the reaction.

[b] Yield of $DBTHSO_2$ after 240 min of the reaction.

[c] TON of DBTH oxidation is calculated as TON_{prim} =[n(DBTH) converted]/[n(Ti)].

[d] Yield of Ph_2SO after 240 min of the reaction.

[e] TON of the primary oxidation of Ph_2S; calculated as TON_{prim}=[n(Ph_2S) converted]/[n(Ti)].

To further investigate the oxidation of Ph_2S to Ph_2SO, a series of experiments over the TS-1-PITi (giving the highest conversion) at different temperatures was conducted. The observed conversion curves are presented in Figure 11. When the temperature was lower from 40 °C being a standard to 30 °C, the conversion decreased nearly to one half after 120 min (47% vs. 25%) on the other hand upon rise of the temperature to 50 °C, the conversion after 120 min increased only to 54%. The Figure 12 shows the selectivity curves obtained in this experiment. The selectivity was determined as the slope of the linear part of the curve up to the conversion of 60%. The selectivity of the experiments conducted at 30 °C and 40 °C was 85%. When the temperature was elevated to 50°C, the selectivity increased to 89%. This suggests that the selectivity of Ph_2S oxidation might be also diffusion driven (as in the case of MPS), only this effect manifests itself at higher temperature.

Figure 11: Conversion curves of oxidation of Ph2S over TS-1-PITi at different temperatures.

Figure 12: Selectivity curves for Ph2SO in oxidation of Ph2S over TS-1-PITi at different temperature.

4. Conclusions

In conclusion, the oxidation of methylphenyl sulphide (MPS), diphenyl sulphide (Ph_2S) and dibenzothiophene (DBTF) over lamellar crystalline titanosilicate catalysts under mild conditions with hydrogen peroxide as the oxidant was investigated. The lamellar titanosilicates provided enhanced activity thanks to easily accessible active sites located on the outer surface of their layers. The selectivity of the MPS oxidation to methylphenyl sulphoxide is driven by the diffusion restrictions in the catalyst. The lower are the diffusion restrictions the higher is the selectivity. The selectivity might be further increased by dosing of the oxidant to keep its concentration low during all the reaction.

The Ti-IPC-1-PI prepared by the postsynthesis modification of Ti-**UTL** provided an outstanding intrinsic activity (TON_{tot} = 1418) together with conversion (e.g. MPS conversion 48% after 120 min) similar to other lamellar titanosilicates (e.g. MPS conversion over layered TS-1 46% after 120 min) in

both MPS and Ph_2S oxidations. The silica-titania pillared TS-1-PITi catalyst showed the highest potential of the tested catalysts to act as an oxo-desulphuration catalyst, easilly oxidising the DBTH to dibenzothiothene sulphone (DBTH conversion 28% after 240 min). On the other hand, conventional zeolites TS-1 and Ti-IPC-2 catalysts did not provide any conversion of DBTH.

Acknowledgement

The authors acknowledge the Czech Science Foundation (P106/12/G015) for the financial support of this research.

References

[1] B.M. Trost, *Bull. Chem. Soc. Jpn.*, 1988, **61**, 107.

[2] H. Satoh, in *Proton Pump Inhibitors: A Balanced View,* eds. T. Chiba, P. Malfertheiner, H. Satoh, Karger, Basel, 2013, 1.

[3] Metabolic Pathways of Agrochemicals: Insecticides and fungicides eds. T. Roberts, D. Hutson, The Royal Society of Chemistry, Cambridge, 1999, 535.

[4] J.M. Fraile, C. Gil, J.A. Mayoral, B. Muel, L. Roldán, E. Vispe, S. Calderón, F. Puente, *Appl. Catal., B,* 2016, **180**, 680.

[5] M.B. Smith, J. March, *March's Advanced Organic Chemistry,* Wiley, New York, 6th ed., 2007, 1780.

[6] S. Vayssié, H. Elias, *Angew. Chem. Int. Ed.,* 1998, **37**, 2088.

[7] M. De Rosa, M. Lamberti, C. Pellecchia, A. Scettri, R. Villano, A. Soriente, *Tetrahedron Lett.*, 2006, **47**, 7233.

[8] C. Bolm, F. Bienewald, *Angew. Chem. Int. Ed.,* 1996, **34,** 2640.

[9] R. Noyori, M. Aoki, K. Sato, *Chem. Commun.*, 2003, 1977.

[10] X.-F. Wu, *Tetrahedron Lett.* 2012, **53**, 4328.

[11] S. Hussain, S.K. Bharadwaj, R. Pandey, M.K. Chaudhuri, *Eur. J. Org. Chem.* 2009, 3319.

[12] A. Corma, P. Esteve, A. Martínez, S. Valencia, *J. Catal.*, 1995, **152,** 18.

[13] A. Corma, U. Diaz, M.E. Domine, V. Fornés, *Chem. Commun.,* 2000, 137.

[14] J. Přech, M. Kubů, J. Čejka, *Catal. Today*, 2014, **227**, 80.

[15] J. Přech, D. Vitvarová, L. Lupínková, M. Kubů, J. Čejka, *Microporous Mesoporous Mater.*, 2015, **212**, 28.

[16] T. Tatsumi, M. Nakamura, S. Negishi, H. Tominaga, *J. Chem. Soc. Chem. Commun.,* 1990, 476.

[17] G. Perego, G. Bellussi, C. Corno, M. Taramasso, F. Buonomo, A. Esposito, *Stud. Surf. Sci. Catal.,* 1986, **28**, 129.

[18] M. Sasaki, Y. Sato, Y. Tsuboi, S. Inagaki, Y. Kubota, *ACS Catal.,* 2014, **4**, 2653.

[19] P. Birke, P. Kraak, R. Schödel, F. Vogt, *Stud. Surf. Sci. Catal.*, 1994, **83**, 425.

[20] L. Wang, Y. Liu, W. Xie, H. Wu, X. Li, M. He, P. Wu, *J. Phys. Chem. C,* 2008, **112**, 6132.

[21] J. S. Reddy, P. A. Jacobs, *Catal. Lett.,* 1996, **37**, 213.

[22] V. Hulea, P. Moreau, F. Di Renzo, *J. Mol. Catal. A: Chem.,* 1996, **111**, 325.

[23] A. Corma, M. Iglesias, F. Sánchez, *Catal. Lett.,* 1996, **39**, 153.

[24] N.N. Trukhan, V.N. Romannikov, A.N. Shmakov, M.P. Vanina, E.A. Paukshtis, V.I. Bukhtiyarov, V.V. Kriventsov, I.Yu. Danilov, O.A. Kholdeeva, *Microporous Mesoporous Mater.*, 2003, **59**, 73.

[25] Y. Kon, T. Yokoi, M. Yoshioka, S. Tanaka, Y. Uesaka, T. Mochizuki, K. Sato, T. Tatsumi, *Tetrahedron*, 2014, **70**, 7584.

[26] W.J. Roth, P. Nachtigall, R.E. Morris, J. Čejka, *Chem. Rev*., 2014, **114**, 4807.

[27] W.J. Roth, *Stud. Surf. Sci. Catal.* 2005, **158**, 19.

[28] Schreyeck, L.; Caullet, P.; Mougenel, J. C.; Guth, J. L.; Marler, B. *J. Chem. Soc. Chem. Commun.* 1995, 2187.

[29] M. Choi, K. Na, J. Kim, Y. Sakamoto, O. Terasaki, R. Ryoo, *Nature*, 2009, **461**, 246.

[30] W.J. Roth, P. Nachtigall, R.E. Morris, P.S. Wheatley, V.R. Seymour, S.E. Ashbrook, P. Chlubná, L. Grajciar, M. Položij, A. Zukal, O. Shvets, J. Čejka, *Nat. Chem.* 2013, **5,** 628.

[31] P. Chlubná-Eliášová, Y. Tian, A.B. Pinar, M. Kubů, J. Čejka, R.E. Morris, *Angew. Chem. Int. Ed.,* 2014, **53**, 7048.

[32] K. Na, Ch. Jo, J. Kim, W. Ahn, R. Ryoo, *ACS Catal.,* 2011, **1**, 901.

[33] W.J. Roth, O.V. Shvets, M. Shamzhy, P. Chlubná, M. Kubů, P. Nachtigall, J. Čejka, *J. Am. Chem. Soc.* 2011, **133**, 6130.

[34] M. Taramasso, G. Perego, B. Notari in *Verified Syntheses of Zeolitic Materials,* ed. H. Robson, Elsevier, Amsterdam, 2nd rev. ed., 2001, 207.

[35] J. Přech, P. Eliášová, D. Aldhayan, M. Kubů, *Catal. Today,* 2015, **243**, 134.

[36] J. Přech, J. Čejka, *Catal. Today,* 2015, DOI: 10.1016/j.cattod.2015.09.036.

[37] O.V. Shvets, N. Kasian, A. Zukal, J. Pinkas, J. Čejka, *Chem. Mater.,* 2010, **22**, 3482.

[38] B.C. Lippens, J.H. de Boer, *J. Catal*., 1965, **4**, 319.

[39] E. Verheyen, L. Joos, K. Van Havebergh, E. Breynaert, N. Kasian, E. Gobechiya, K. Houthoofd, C. Martineau, M. Hinterstein, F. Taulelle, V. Van Speybroeck, M. Waroquier, S. Bals, G. Van Tendeloo, C.E.A Kirschhock, J.A. Martens, *Nature Mater.*, 2012**, 11**, 1059.

[40] A. Zecchina, G. Spoto, S. Bordiga, A. Ferrero, G. Petrini, G. Leofanti, M. Padovan, *Stud. Surf. Sci. Catal.,* 1991, **69**, 251.

[41] P. Wu, T. Tatsumi, T. Komatsu, T. Yashima, *J. Phys. Chem. B,* 2001, **105,** 2897.

[42] P. Ratnasamy, V.N. Shetti, P. Manikandan, D. Srinivas, *J. Catal.*, 2003, **216**, 461.

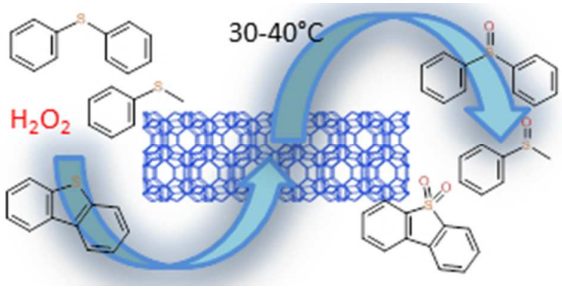

79x39mm (96 x 96 DPI)

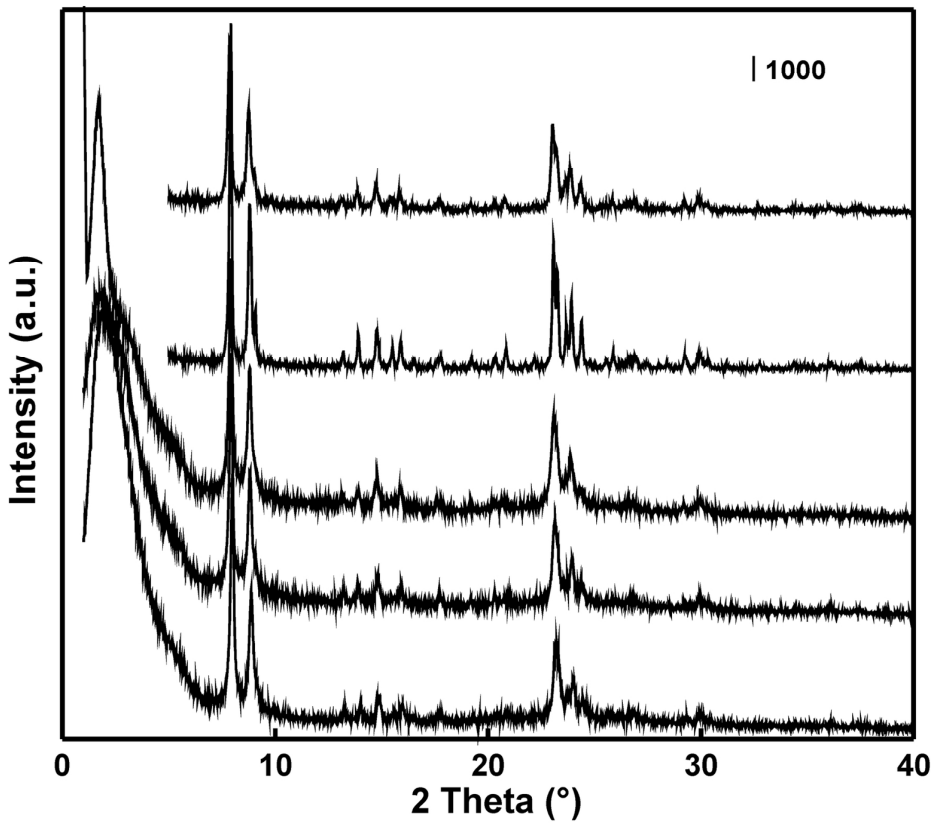

75x68mm (600 x 600 DPI)

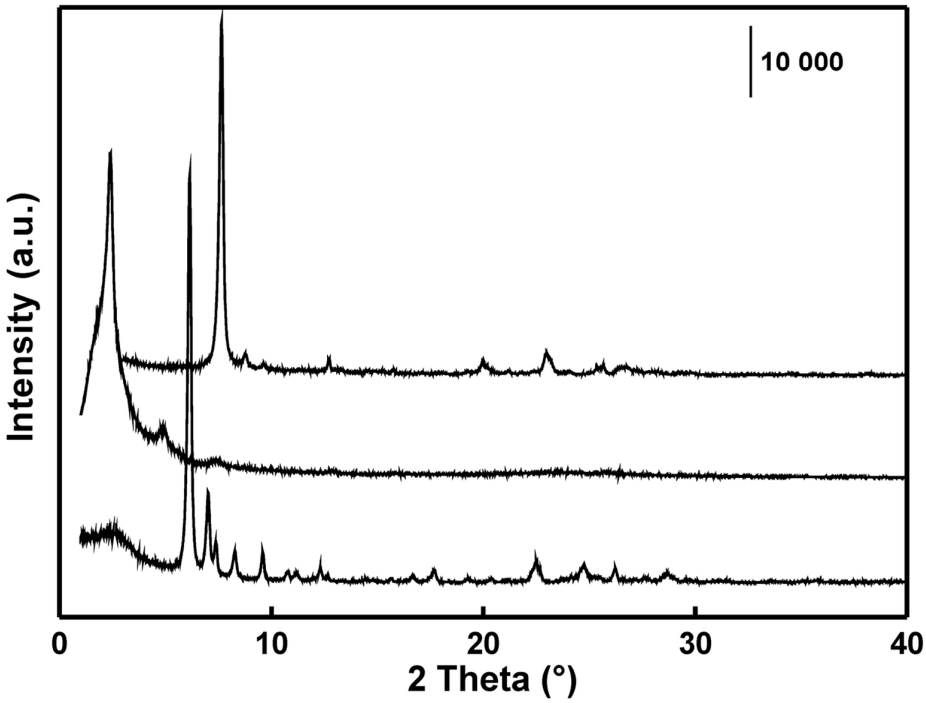

64x50mm (600 x 600 DPI)

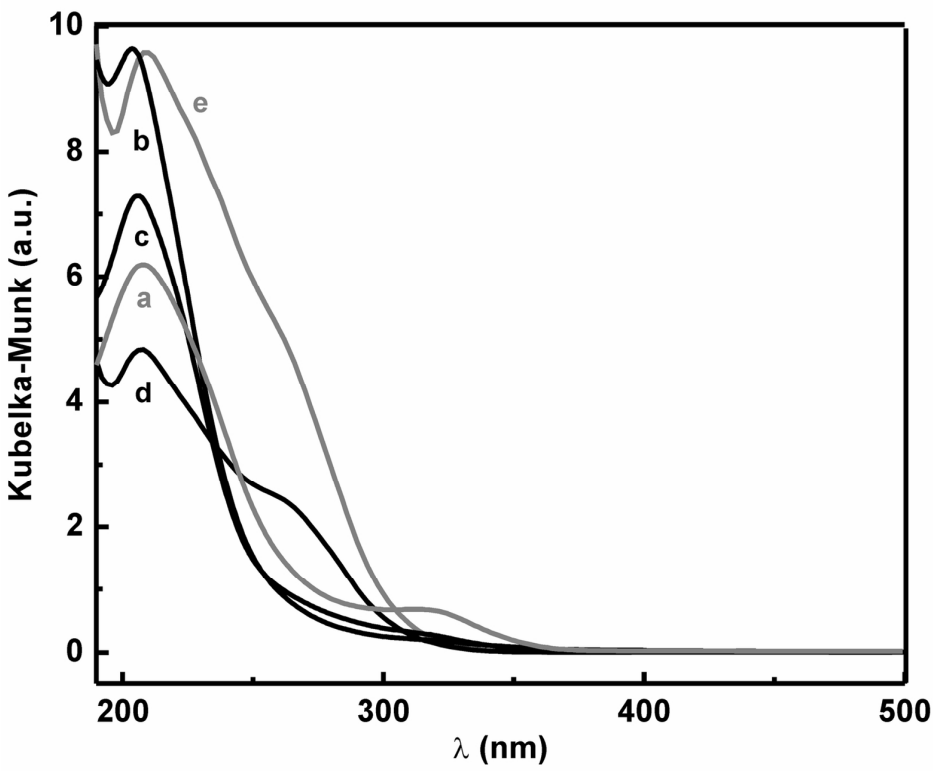

69x57mm (600 x 600 DPI)

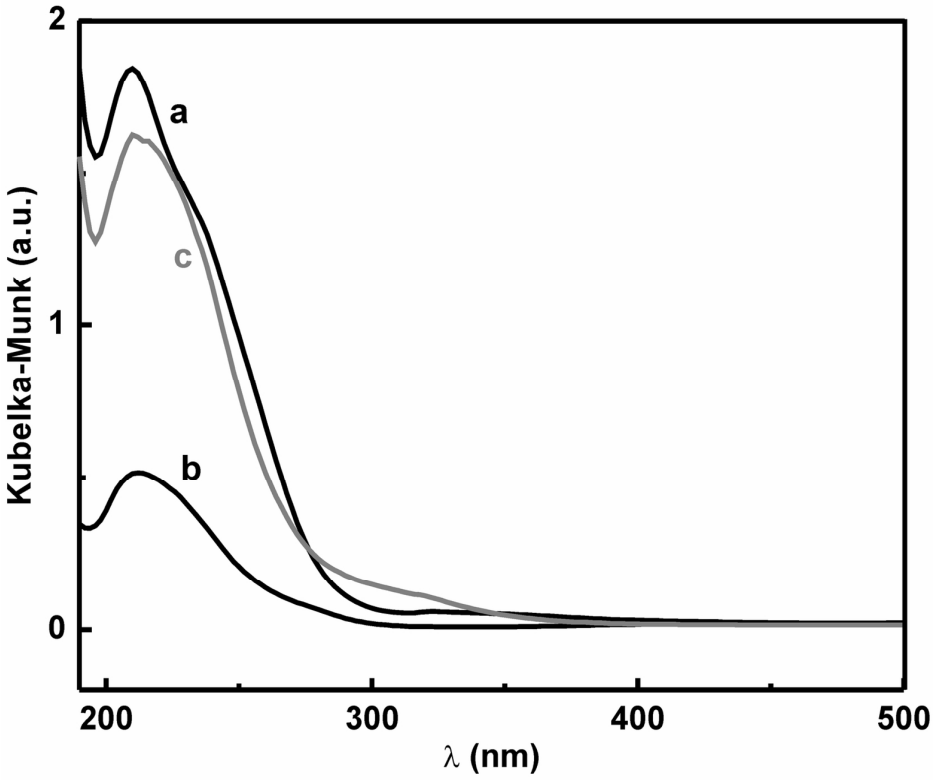

70x60mm (600 x 600 DPI)

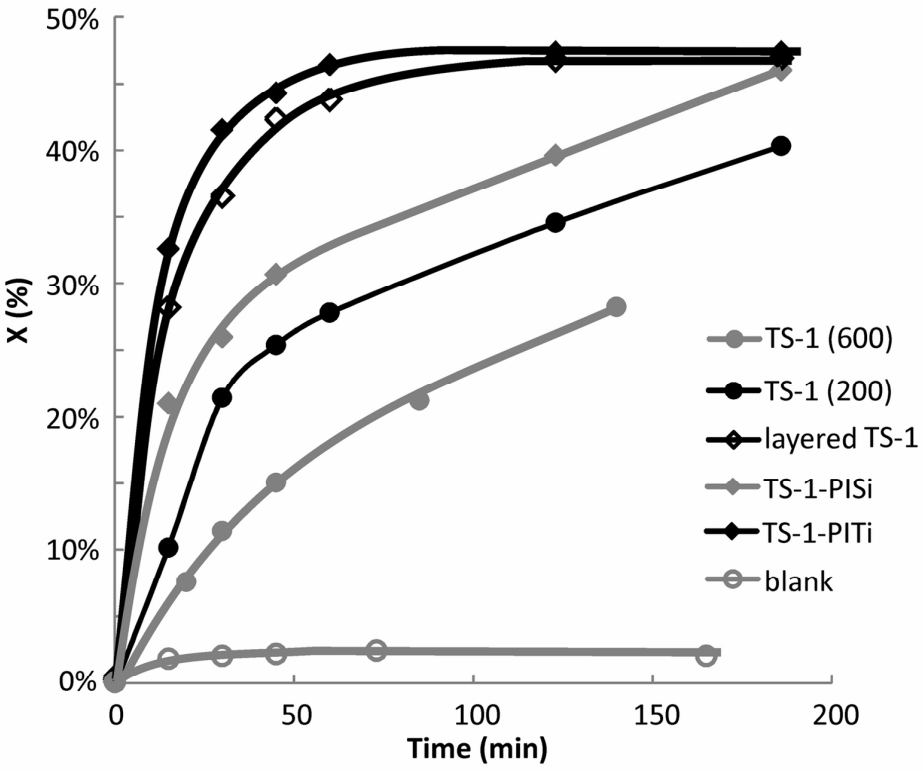

69x57mm (600 x 600 DPI)

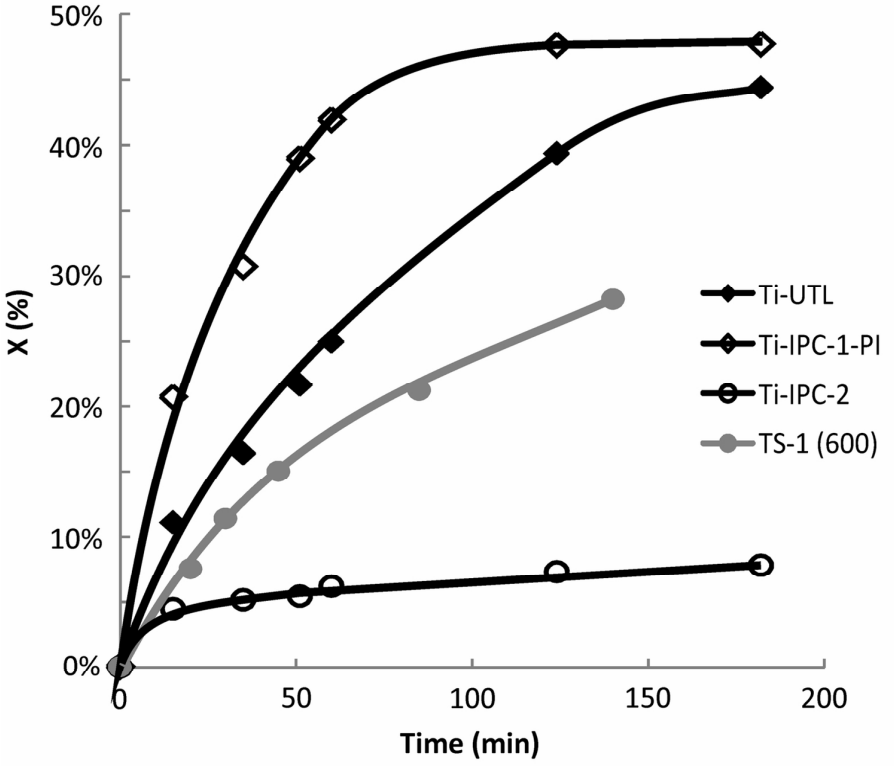

68x56mm (600 x 600 DPI)

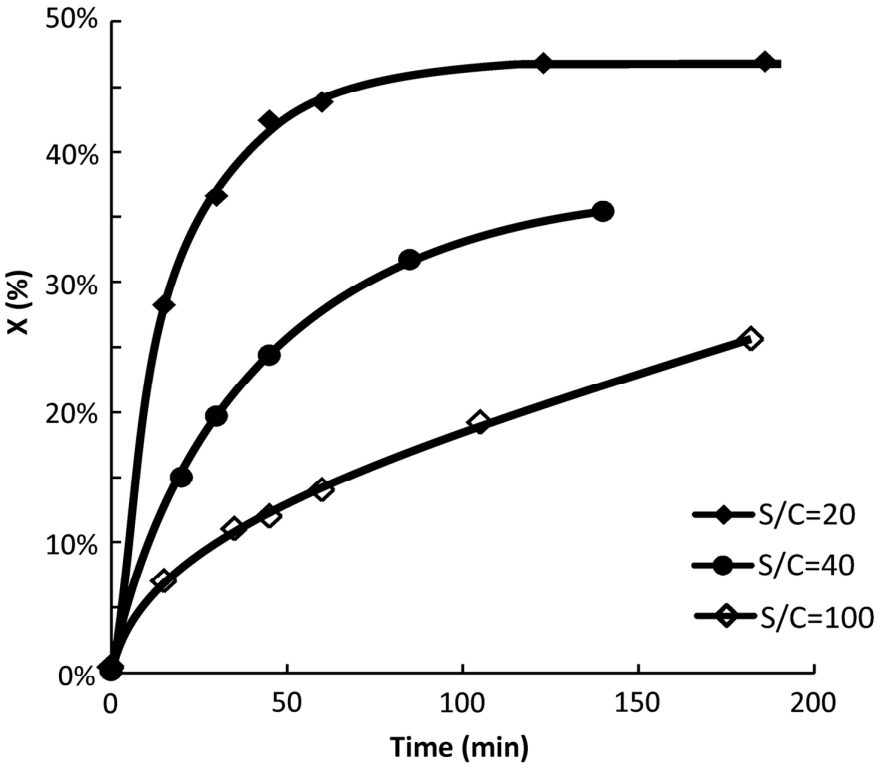

69x57mm (600 x 600 DPI)

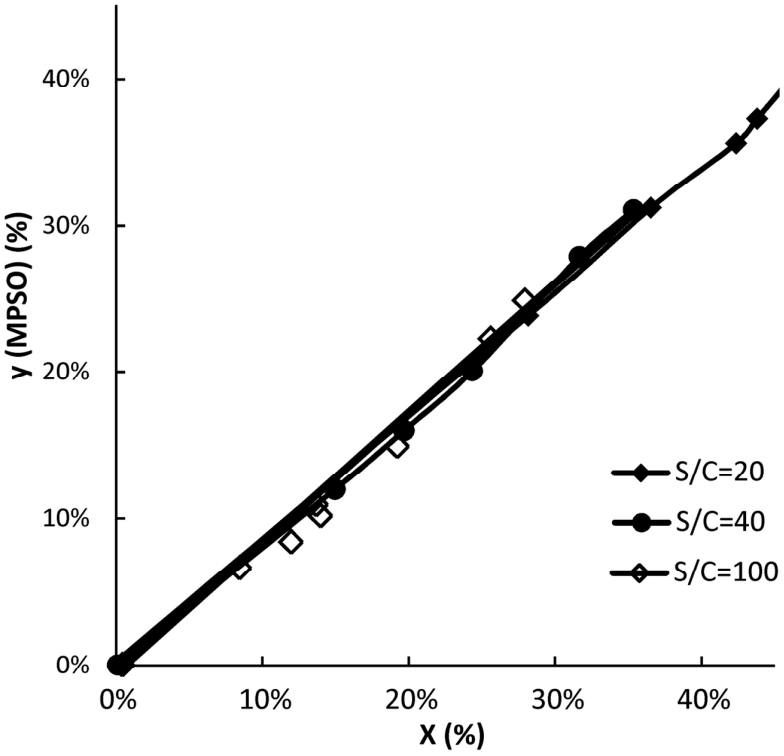

68x57mm (600 x 600 DPI)

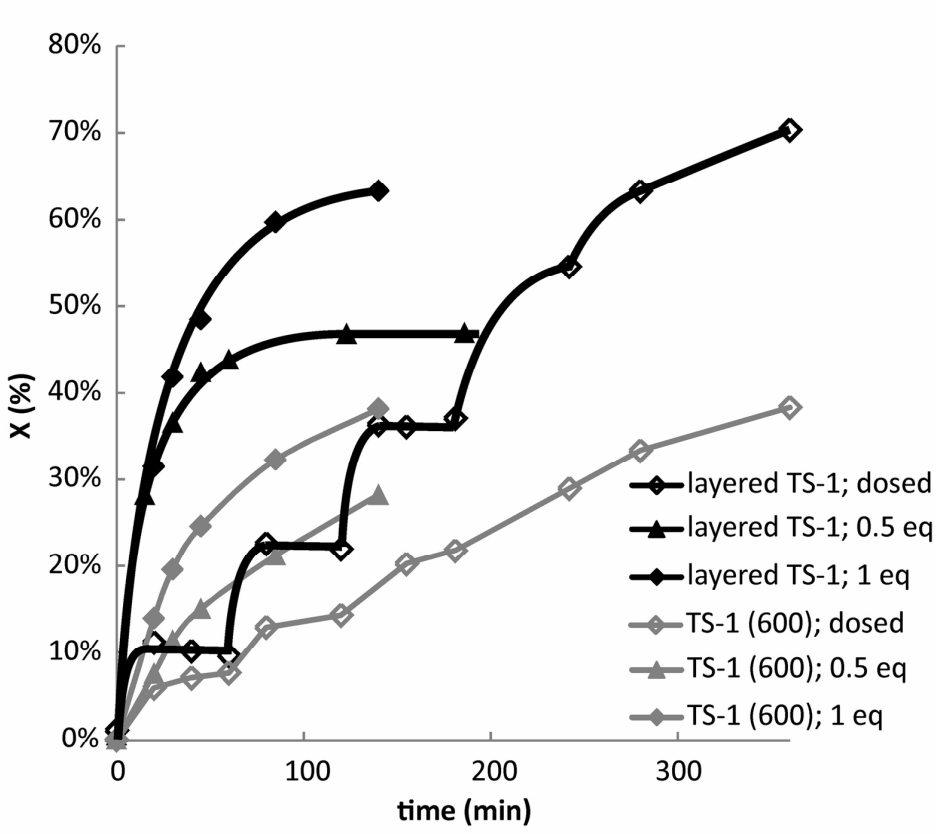

74x66mm (600 x 600 DPI)

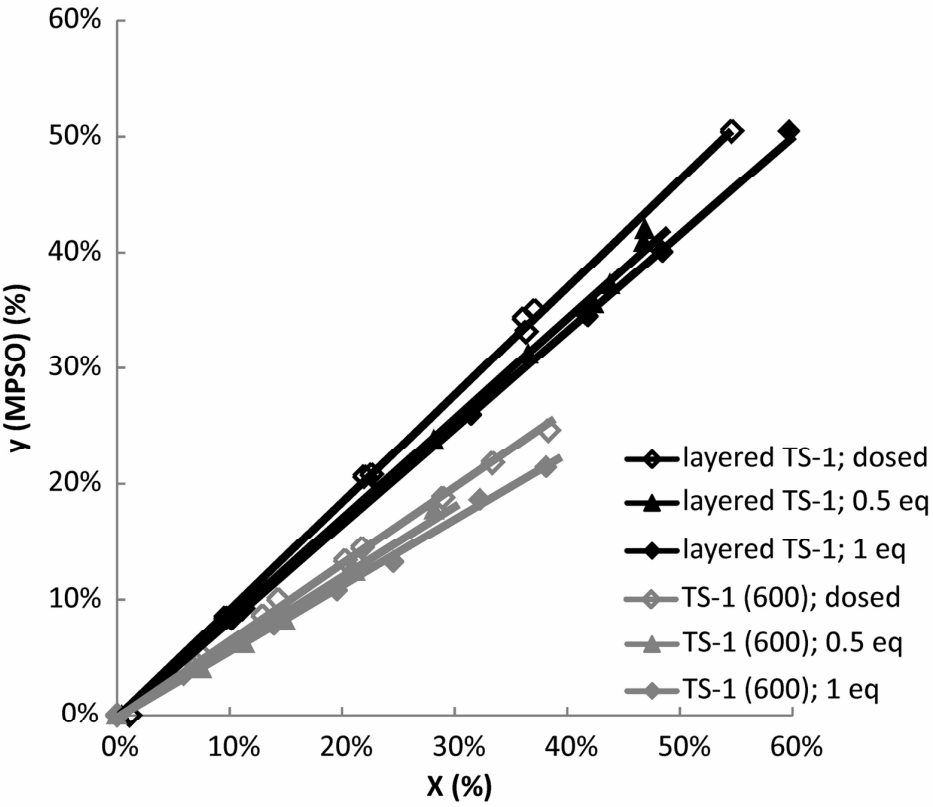

72x62mm (600 x 600 DPI)